

Investigation of Combination Effect Between 6 MV X-Ray Radiation and Polyglycerol Coated Superparamagnetic Iron Oxide Nanoparticles on U87-MG Cancer Cells

Jafari S.^{1*}, Cheki M.², Tavakoli M. B.³, Zarrabi A.⁴, Ghazikhanlu Sani K.¹, Afzalipour R.⁵

ABSTRACT

Background: Radiosensitization using nanoparticles is proposed as a novel strategy for treatment of different cancers. Superparamagnetic iron oxide nanoparticles (SPIONs) have been reported to enhance effects of radiotherapy in several researches.

Objective: The objective of this research is to investigate the radiosensitization properties of polyglycerol coated SPIONs (PG-SPIONs) on U87-MG cancer cells.

Material and Methods: In this experimental study, polyglycerol coated SPIONs were synthesized by thermal decomposition method and characterized by FTIR, TEM and VSM analysis. Cellular uptake of nanoparticles by cells was examined via AAS. Cytotoxicity and radiosensitization of nanoparticles in combination with radiation were evaluated by MTT and colony assay, respectively.

Results: Mean size of nanoparticles was 17.9 ± 2.85 nm. FTIR verified SPIONs coating by Polyglycerol and VSM showed that they have superparamagnetic behaviour. Viability significantly ($P < 0.001$) decreased at concentrations above $100 \mu\text{g/ml}$ for SPIONs but not for PG-SPIONs ($P > 0.05$). Dose verification results by TLD for doses of 2 and 4 Gy were 2 ± 0.19 and 4 ± 0.12 Gy respectively. The combination index for all situations was less than 1 and the effect is antagonism.

Conclusion: However, PG-SPIONs combination with 6 MV X-ray reduced survival of U87-MG cells compared to radiation alone but the effect is antagonism.

Citation: Jafari S, Cheki M, Tavakoli M. B, Zarrabi A, Ghazikhanlu Sani K, Afzalipour R. Investigation of Combination Effect Between 6 MV X-Ray Radiation and Polyglycerol Coated Superparamagnetic Iron Oxide Nanoparticles on U87-MG Cancer Cells. *J Biomed Phys Eng*. 2020;10(1):15-24. doi: 10.31661/jbpe.v0i0.929.

Keywords

Polyglycerol; X-Rays; Magnetite Nanoparticles

Introduction

Combination of radiotherapy with nanoparticles as radiosensitizer agents is proposed for treatment of cancers in different studies [1-6]. Radiotherapy plays an important role in treatment of cancers. About fifty percent of cancers are currently treated by this modality [7]. Radiotherapy goal is to kill all cancer cells with no damage to soft tissues [8]. Many efforts have been made in radiation dose delivery techniques to achieve this goal, but there are still inefficiencies which prevent some cancers such as Glioblastoma Multiforme (GBM) being

¹PhD, Department of Radiology Technology, School of Paramedicine, Hamadan University of Medical Sciences, Hamadan, Iran

²PhD, Department of Radiologic Technology, Faculty of Paramedicine, Ahvaz Jundishapur University of Medical Sciences, Ahvaz, Iran

³PhD, Department of Medical Physics, School of Medicine, Isfahan University of Medical Sciences, Isfahan, Iran

⁴PhD, Department of Biotechnology, Faculty of Advanced Sciences and Technologies, University of Isfahan, Isfahan, Iran

⁵PhD, Department of Medical Physics, School of Medicine, Iran University of Medical Sciences, Tehran, Iran

*Corresponding author:
S. Jafari
Department of Radiology Technology, School of Paramedicine, Hamadan University of Medical Sciences, Hamadan, Iran
E-mail: Salman.Jafari21@gmail.com

Received: 19 April 2018
Accepted: 8 May 2018

treated to the full [9, 10]. GBM is the most malignant and frequent primary malignancy of the brain which has remained as a clinical unsolved problem [11-14]. The prognosis for GBM is really poor [15, 16].

A standard method for treatment of GBM is currently surgery followed by radiotherapy and concurrent chemotherapy. However, there are some limitations such as remaining of residual malignant cancer cells in the tumor site after surgery, insufficient dose of radiation to the cancer cells and resistance of tumor cells to radiotherapy [17]. Radiation dose for treatment of GBM is usually 60 Gy delivered in 30 fractions [18]. This dose is not sufficient to destroy all cancer cells and increasing dose is generally associated with a rise in soft tissues injures [19, 20].

Among different ways which are suggested to overcome these limitations, nanoparticles have attracted a lot of attention to themselves [21]. Superparamagnetic iron oxide nanoparticles (SPIONs) seem to be a good option for treatment of GBM due to their capability for drug delivery, diagnosis, radiosensitization, biocompatibility and selective targeting under the direction of an external magnetic field [22-25]. SPIONs were reported to enhance the effect of radiation on cancer cells in several studies [3, 26, 27]. Klein et al. studied the effect of combining SPIONs with X-ray on MCF-7 cells and expressed that citrate coated SPIONs are excellent radiosensitizers which enhance the generation of reactive oxygen species (ROS) about 240% [27]. Iron atomic number is relatively high compared to soft tissue which causes increasing X-ray absorption and radiosensitization of cancer cells [28]. Some damage to cancer cells has been reported by iron oxide nanoparticles combination with ionizing radiation [26].

Coating SPIONs by a biocompatible material has several advantages such as prevention of agglomeration with itself [29-31]. Hyperbranched Polyglycerol (HPG) is proposed as a suitable coating agent for SPIONs [32, 33].

It exhibits the great promise in the area of nanoparticles coating material even superior to PEG as reported by Deng et al [34]. In this study, we aimed to synthesize Polyglycerol coated SPIONs (PG-SPIONs) and examine their cytotoxicity and synergistic effects between megavoltage X-ray combination and these nanoparticles in order of cancer treatment.

Material and Methods

Nanoparticles synthesis and characterization

In this experimental study, nanoparticles were synthesized based on polyol process [32]. 0.53 gr of $\text{Fe}(\text{acac})_3$ (Merk) was mixed with 30 ml TREG(PVT.LTD). After stirring under gentle pressure of nitrogen the mixture gradually heated until reflux temperature [35]. When reflux is completed, solvent color goes to dark black. Then sediment is freeze-dried (VaCo5 ZIRBUS) [36]. To coat, 0.5 ml Glycidol monomer was mixed with 15 mg dried SPIONs while stirring at constant temperature 284°F for 1200 minutes [32]. PG-SPIONs sediment then dialyzed using a dialyze bag with a cut-off of 12 kDa.

Transmission microscope (TEM) (Leo 912 AB) images were taken from PG-SPIONs to determine their size and morphology. A program was written on MATLAB(R 2009a) software in order of getting size distribution and mean size of nanoparticles using TEM images. Fourier transform infrared (FT-IR) (JACSO 6300 FT-IR spectrometer) with a resolution of 4 cm^{-1} was taken from PG coated SPIONs to show what groups are included in them. A little amount of SPIONs and PG coated SPIONs were mixed with potassium bromide (KBr) to form a tablet for analysis. Magnetic property of SPIONs is important for biological applications. SPIONs treat such as they become magnetic in the presence of a magnetic field and loss their magnetic properties in the absent of it immediately [37, 38]. To define magnetic

properties of nanoparticles, vibrating sample magnetometer (VSM) (Meghnatis daghigh kavir kashan) was taken. About 100 mg NPs was used for this analysis.

Biological tests

U87-MG cells line was obtained from Pasteur institute of Iran. The cells were grown in T-25 flasks containing culture medium with high glucose DMEM, 10% fetal bovine serum (FBS) and 1% penicillin/streptomycin. Flasks were maintained in an incubator (BINDER) under 5% CO₂ pressure at 37°C temperature. When cells well grew and reached to a suitable confluence, they were separated from the flask floor by 0.25 % trypsin/EDTA solution and were counted for biological tests.

MTT Assay

MTT test was used to examine the cytotoxicity of SPIONs and PG-SPIONs on U87-MG cells. First, the cells were cultured in 12-well plates at the concentrations of 20000 cells in each well. Five groups were chosen to examine cytotoxicity of nanoparticles at different concentrations including 5, 25, 50, 100 and 200µg/ml and one group was left as a control group without any nanoparticles. For each concentration, three wells were cultured. Nanoparticles containing medium were filtered through 0.2 µl filter before addition to wells. After removing nanoparticle-free medium, U87-MG cells were washed twice with PBS and incubated for 24, 48 and 72 hours after adding SPIONs or PG-SPIONs containing medium. After removing a consumed medium, 200 µl MTT solution (nutrient medium containing 5mg/ml 3-(4,5-dimethylthiazol-2-yl)-2,5-diphenyltetrazolium bromide) was added to each well and remained in an incubator for 4 hours at 37°C. Next, the supernatant was carefully taken and 440 µl DMSO was used to dissolve the formazan salt in each well. Cells viability was examined by measuring light absorbance of the solution using 96-well plates. Reading was performed by a microplate reader (BIO-

RAD Model 680) at the wavelength 570nm. The percentage of optical density reading for treated cells with nanoparticles divided by the same for untreated cells was considered to be the cells viability.

For cytotoxicity evaluation of 6 MV X-ray on U87-MG cancer cells, they were irradiated using Anchor accelerators located at Milad Hospital of Isfahan. A number of 20000 cells per each well (24-well plate) were exposed to doses of 1, 2, 4 and 6 Gy in a 20×20 cm² field at the percentage depth dose of 97.8. Dose calculation was performed using PDD table of the accelerator and 5 cm thickness backscatter. Plexiglas acrylic sheets were placed under plates to ensure that the dose is uniform through the irradiated field. MTT assay was performed such as that done for SPIONs and PG-SPIONs. In order to ensure correct radiation dose delivering to cells, dose verification was performed for doses of 2 and 4 Gy using thermoluminescent dosimeter (TLD-100). Two TLDs were embedded in water resistance bags and placed in water filled well shown in (Figure 1) under the field of radiation with the same conditions for cell containing plates. Kruskal-Wallis test was used for statistical analysis of the MTT test results.

Colony assay

To prevent cancer cells from recurring, killing of those cells which can form a colony is very important [39]. Colony assay as a gold



Figure 1: Dose verification using TLD-100 dosimeters.

standard method is usually performed to investigate survival of irradiated or treated cancer cells [40-42]. A number of 50000 cells per each well (12-well plate) were treated by PG-SPI-ONs at the concentration of 100µg/ml after removing the cultured medium. Cells were then exposed to doses of 1, 2, 4 and 6 Gy at room temperature. X-ray irradiation was performed by 6 MV X-ray with output of 1cGy/MU. Irradiated cells then were carefully counted and numbers of 1000 or 2000 cells were cultured in 60 mm petri dishes in triplicate. After irradiation, cells were left in an incubator for 14 days. After removing consumed medium, petri dishes were washed twice by PBS. Colonies were fixed by formaldehyde and stained with 5% crystal violet in PBS. Colonies which had more than 50 cells were counted and a survival fraction was determined for each group by the equation 1 [41].

$$\text{The survival fraction} = \frac{\text{number of colonies after treatment}}{\text{number of cells seeded} \times \text{PE}} \quad (1)$$

Which PE (plating efficiency) is the ratio of the number of colonies to the number of cells seeded (equation 2):

$$PE = \frac{\text{number of colonies formed}}{\text{number of cells seeded}} \times 100 \quad (2)$$

To determine combination effects between radiation and nanoparticles, Chou analysis was performed using compusyn software [43].

The combination index (CI) was used to determine if the effect is synergistic or antagonistic. CI less than 1 and greater than 1 indicates synergistic and antagonistic, respectively.

Cellular uptake of nanoparticles determined using atomic absorption spectroscopy (AAS). Cells were first cultured and washed twice with PBS. A numbers of 2×10^6 cells were counted and transferred to 60 mm petri dishes and placed in an incubator for 24 hours. PG-SPI-ONs at concentrations 1, 2 and 3 mg/ml were added to the cells and placed in an incubator for 2 days, then washed with PBS three times and trypsinized.

After centrifuging, the remaining cells in bottom of falcons were used for AAS. 1.5 ml Aqua regia were added to the cells in each falcon and the final volume of deionized water increased to 5 ml. The falcons were placed in a water bath under 45°C temperature for 4 h and the digested homogenate was centrifuged at 19400g. The supernatant was used for AAS. The measurements were performed using PERKIN-ELMER AAS following calibration process.

Results

Nanoparticles characterization

PG-SPI-ONs shape and size distributions are shown in Figure 2a and b, respectively. Mean

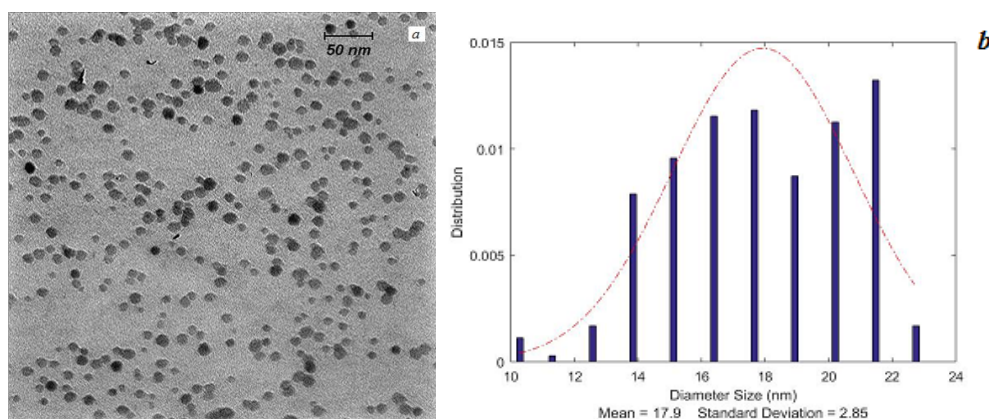


Figure 2: (a) Transmission electron microscopy of PG-SPI-ONs and (b) their size distributions.

diameter of PG coated SPIONS was 17.9 ± 2.85 nm. They have a spherical morphology.

Figure 3 shows FTIR spectrum of undialyzed PG-SPIONS. The presence of the peaks related to C-O-C and C-H bonds is clearly seen on the spectrum. In this case, SPIONS have been coated with polyglycerol successfully. Peak related to glycidol has been removed from FTIR spectrum by the dialyze bag.

Figure 4 shows magnetic properties of nanoparticles. Saturation magnetization for SPIONS is greater than PG-SPIONS [20].

Viability tests

U87-MG cells pictures which have taken

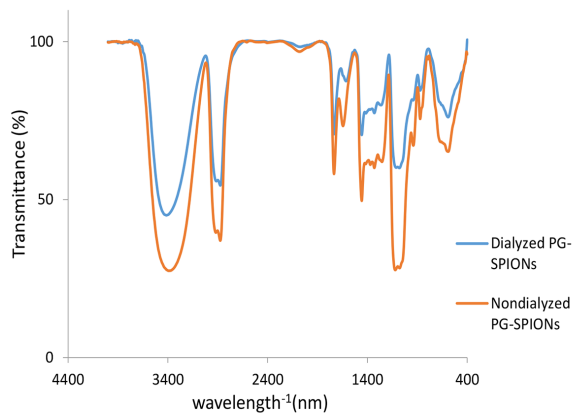


Figure 3: Dialyzed and undialyzed PG-SPIONS FTIR.

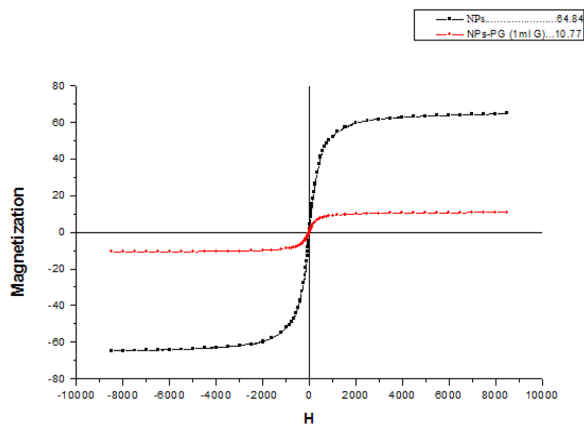


Figure4: Magnetic properties of nanoparticles.

by an inverted microscope (Nikon Eclipse - TS100) with different magnifications are shown in Figure 5 from part (a) to (f). Cells degradation is seen in this figure part c and d. Cells colony is obviously shown in part e and f.

Cytotoxicity of treated cells with SPIONS, PG-SPIONS, 6 MV X-ray and their combination were evaluated by MTT assay. Figures 6-8 show viability percent of U87-MG cells treated with SPIONS and PG-SPIONS incubated for 24, 48 and 72 hours, respectively. Viability significantly ($P < 0.001$) decreases at concentrations above $100\mu\text{g/ml}$ for SPIONS in all times but it does not differ for PG-SPIONS. ($P > 0.05$).

Figure 9 shows viability percent of U87-MG cells irradiated with doses of 1, 2, 4 and 6 Gy

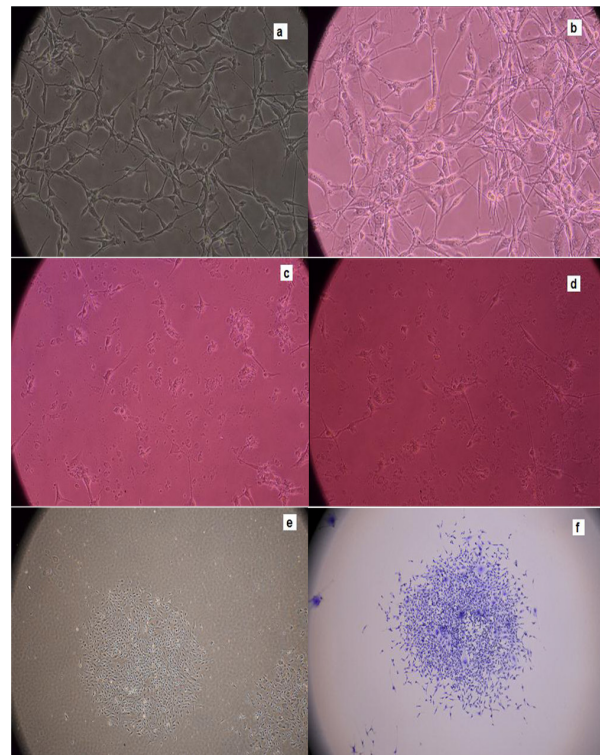


Figure 5: U87-MG cells pictures (a) 48 h post culturing (b) after treating with PG-SPIONS (c) exposed to 6 Gy radiation dose (d) treated with PG-SPIONS and exposed to dose 6 Gy radiation dose (e) colony formed and (f) stained colonies for counting.

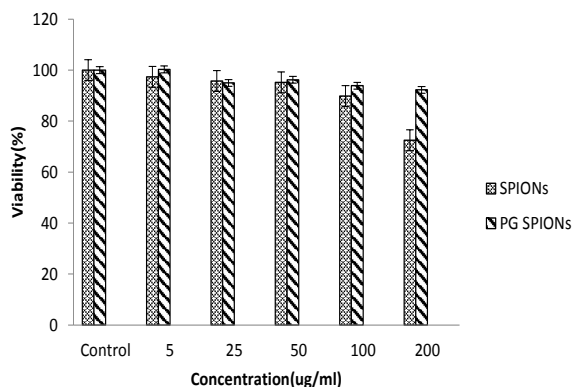


Figure 6: Measured viability for U87-MG cancer cells treated with SPIONs and PG-SPIONs for incubation time of 24h.

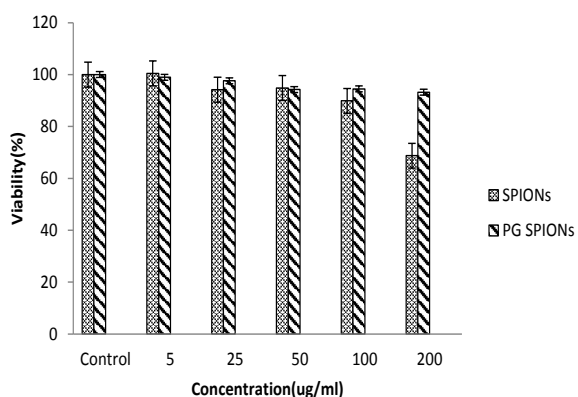


Figure 7: Measured viability for U87-MG cancer cells treated with SPIONs and PG-SPIONs for incubation time of 48h.

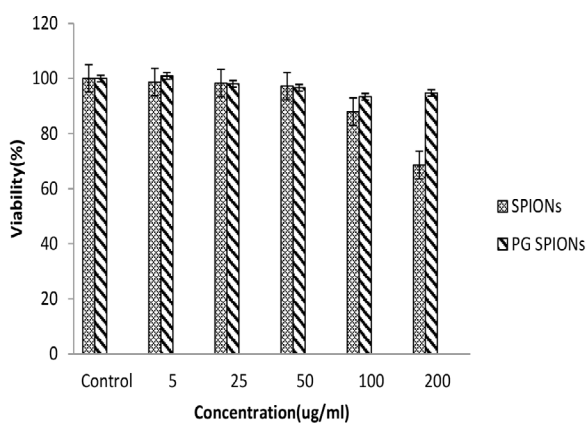


Figure 8: Measured viability for U87-MG cancer cells treated with SPIONs and PG-SPIONs for incubation time of 72h.

from 6 MV X-ray. Viability decreases significantly ($P < 0.001$) with increasing radiation dose. Dose verification results by TLD for irradiation of 2 and 4 Gy to cancer cells were 2 ± 0.19 and 4 ± 0.12 Gy respectively.

Colony assay results are shown by dose response curves which consist of a vertical axis with a logarithmic scale to determine a survival fraction and a horizontal axis defining radiation doses. The survival curve for combination of 6 MV X-ray and PG-SPIONs at the concentration 100 ug/ml is shown in Figure 10. Reduction in the survival fraction by dose increasing for combination of nanoparticles with radiation is greater than radiation alone but it is not significant ($P > 0.05$).

Results of combination index calculation of PG-SPIONs combination with 6 MV X-ray showed that for all situations CI was less than 1 and the effect is antagonistic.

AAS results are shown in Figure 11. Cellular uptake of nanoparticles increased with higher doses of nanoparticles ($P < 0.05$) but for all concentrations the uptake is relatively low.

Discussion

In this study we were going to synthesize PG coated SPIONs in order to increase radiosensitivity of U87-MG cancer cells. Results showed that size and size distribution of our nanoparticles are suitable for biomedical applications. As expected, magnetization of PG-SPIONs decreased compared to SPIONs. This situation is seen at other researches [26, 44, 45]. This can be due to coating of SPIONs with Polyglycerol which reduces SPIONs concentration for analysis and magnetization consequently [46]. There is a good agreement between our results with Martin et al [45]. Strong peaks on FTIR spectrum in our study indicated successful coating of SPIONs by polyglycerol which already has been reported by Wang et al [47].

For uncoated SPIONs, cells viability significantly ($P < 0.001$) decreases at concentrations above $100 \mu\text{g/ml}$. This result is also reported in

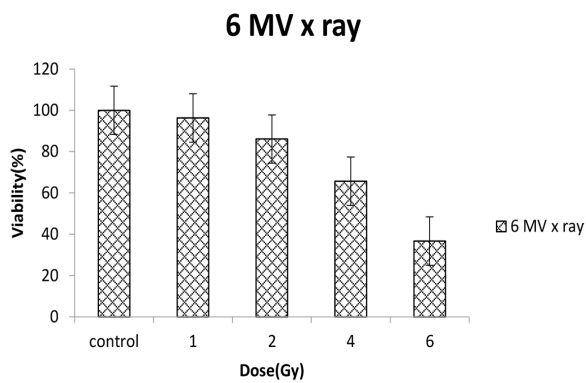


Figure 9: Measured viability for U87-MG cancer cells exposed to doses of 1, 2, 4 and 6 Gy from 6 MV X rays.

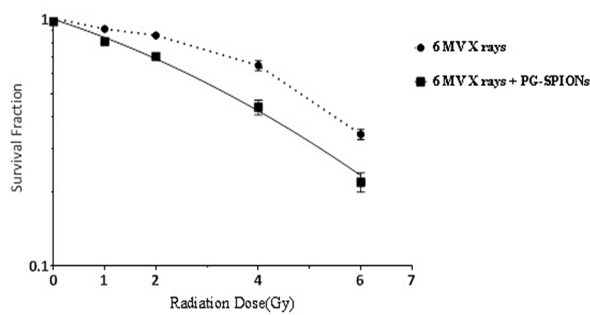


Figure 10: Survival curve for U87-MG cancer cells treated with combination of 6 MV X rays and PG-SPIONs at concentration of 100ug/ml.

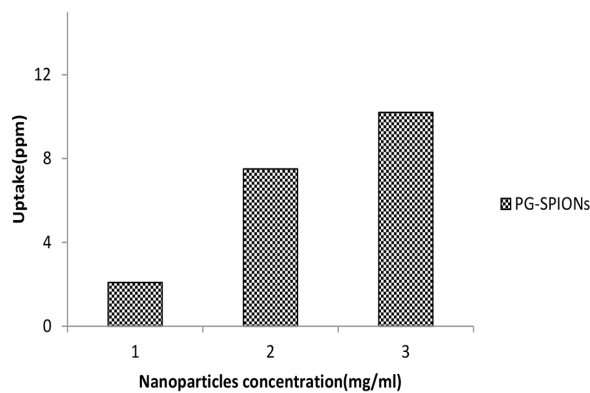


Figure 11: PG-SPIONs uptake by U87-MG cancer cells treated with doses of 1, 2 and 3 mg/ml nanoparticles.

other similar studies [48-50]. Ankamwar et al, have reported that SPIONs at low concentrations have no cytotoxicity effects on U87-MG cancer cells but obvious cytotoxicity is seen at concentration of 100 ug/ml [48]. Entry of SPIONs into cancer cells leads to formation of reactive oxygen species (ROS) such as H_2O_2 , OH^\bullet and anion superoxides ($O_2^{\bullet-}$) which in turn causes oxidative stress and toxicity in cells [51]. Viability for U87-MG cells treated with PG-SPIONs is higher compared with SPIONs. Despite of SPIONs, viability did not decrease by increasing concentrations of PG-SPIONs ($P > 0.001$). In other studies cytotoxicity is not reported even for higher concentrations of PG-SPIONs [52]. Saatchi et al, examined cytotoxicity of PG coated gallium on HUVEC cancer cells and the results showed no significant toxicity effects at the concentration of 10 mg/ml [53]. Low uptake of PG-SPIONs by U87-MG cells can be attributed to the surface hydrophilicity of nanoparticles [47].

U87-MG cancer cells viability significantly ($P < 0.001$) decreased by increasing radiation doses. Radiation interaction with cancer cells can damage DNA directly or produce free radicals by radiolysis of water molecules that in turn is destructive and kills the cells [54, 55]. Reactive oxygen species (ROS) are generated as a result of reactions free radicals with biological molecules which cause oxidation of lipids, protein and DNA that induce apoptotic and necrotic cell death due to mitochondrial dysfunction [56, 57].

SPIONs aggregations on cell membrane cause a membrane lipid peroxidation and improve radiosensitization [58]. Klein et al, expressed that production of ROS increased in SPIONs loaded with MCF-7 cells exposed to X-ray increased compared with cells only exposed to X-ray. The ROS production was explained to be related with release of iron ions into the cytosol where immediate chelation by citrate or adenosine phosphate will take place and active surface of nanoparticles as catalyst for the Haber-Weiss cycle [27, 59, 60]. ROS

production increases with a rise in iron ions in cancer cells which in turn leads to more cellular cytotoxicity [1]. Synergy is that the effect of two agents given together is more effective than would be predicted based on their individual activity; If agent 1 alone reduces the surviving fraction to 0.5 and agent 2 used alone also reduces survival to 0.5, the combination effect will be synergistic if it is less than 0.25 [61]. Combination of PG-SPIONs with 6 MV X-ray reduced survival fractions of U87-MG cells compared to radiation alone but difference was not significant ($P > 0.05$). Although radiosensitization of SPIONs alone and with different coating has been reported in different studies, but in our study the radiation effect enhancement property of these nanoparticles was not considerable. It may be related to the coating material of HPG. Results of MTT assay for PG-SPIONs confirm this because viability did not significantly decrease compared to SPIONs alone even at high concentrations of nanoparticles. The mechanisms underlying radiosensitization are still incompletely understood and more studies are needed to be conducted with this regards.

Conclusion

This study revealed that PG-SPIONs are not cytotoxic on U87-MG cancer cells even at concentrations up to 200 $\mu\text{g/ml}$. Results of MTT test showed that cell viability decreases significantly by increasing radiation doses. Based on our result, we can conclude that PG-SPIONs combination with 6 MV X-ray reduced survival of U87-MG cells, it is not a good radiosensitizer to be used for radiotherapy.

Acknowledgment

We thank Hamadan and Isfahan Universities of medical sciences and biotechnology laboratory of Isfahan University for their kindly supports.

Conflict of Interest

None

References

- Huang G, Chen H, Dong Y, Luo X, Yu H, Moore Z, et al. Superparamagnetic iron oxide nanoparticles: amplifying ROS stress to improve anticancer drug efficacy. *Theranostics*. 2013;3:116-26. doi: 10.7150/thno.5411. PubMed PMID: 23423156. PubMed PMCID: PMC3575592.
- Babaei M, Ganjalikhani M. The potential effectiveness of nanoparticles as radio sensitizers for radiotherapy. *Bioimpacts*. 2014;4:15-20. doi: 10.5681/bi.2014.003. PubMed PMID: 24790894. PubMed PMCID: PMC4005278.
- Khoei S, Mahdavi SR, Fakhimikabir H, Shakeri-Zadeh A, Hashemian A. The role of iron oxide nanoparticles in the radiosensitization of human prostate carcinoma cell line DU145 at megavoltage radiation energies. *Int J Radiat Biol*. 2014;90:351-6. doi: 10.3109/09553002.2014.888104. PubMed PMID: 24475739.
- Su XY, Liu PD, Wu H, Gu N. Enhancement of radiosensitization by metal-based nanoparticles in cancer radiation therapy. *Cancer Biol Med*. 2014;11:86-91. doi: 10.7497/j.issn.2095-3941.2014.02.003. PubMed PMID: 25009750. PubMed PMCID: PMC4069802.
- Retif P, Pinel S, Toussaint M, Frochet C, Chouikrat R, Bastogne T, et al. Nanoparticles for Radiation Therapy Enhancement: the Key Parameters. *Theranostics*. 2015;5:1030-44. doi: 10.7150/thno.11642. PubMed PMID: 26155318. PubMed PMCID: PMC4493540.
- Haume K, Rosa S, Grellet S, Smialek MA, Butterworth KT, Solov'yov AV, et al. Gold nanoparticles for cancer radiotherapy: a review. *Cancer Nanotechnol*. 2016;7:8. doi: 10.1186/s12645-016-0021-x. PubMed PMID: 27867425. PubMed PMCID: PMC5095165.
- Delaney GP, Barton MB. Evidence-based estimates of the demand for radiotherapy. *Clin Oncol (R Coll Radiol)*. 2015;27:70-6. doi: 10.1016/j.clon.2014.10.005. PubMed PMID: 25455408.
- Eriksson D, Stigbrand T. Radiation-induced cell death mechanisms. *Tumour Biol*. 2010;31:363-72. doi: 10.1007/s13277-010-0042-8. PubMed PMID: 20490962.
- Amelio D, Amichetti M. Radiation therapy for the treatment of recurrent glioblastoma: an overview. *Cancers (Basel)*. 2012;4:257-80. doi: 10.3390/cancers4010257. PubMed PMID: 24213239. PubMed PMCID: PMC3712688.
- Raizer J, Parsa A. Current understanding and treatment of gliomas: Springer; 2015.
- Huynh GH, Deen DF, Szoka Jr FC. Barriers to carrier mediated drug and gene delivery to brain tumors. *J Control Release*. 2006;110:236-59. doi: 10.1016/j.jconrel.2005.09.053. PubMed PMID: 16318895.
- Invernici G, Cristini S, Alessandri G, Navone SE, Canzi L, Tavian D, et al. Nanotechnology advances in brain tumors: the state of the art. *Recent Pat Anti-cancer Drug Discov*. 2011;6:58-69. PubMed PMID:

- 21110824.
13. Rozhkova EA. Nanoscale materials for tackling brain cancer: recent progress and outlook. *Adv Mater.* 2011;**23**:H136-50. doi: 10.1002/adma.201004714. PubMed PMID: 21506172.
 14. Ling Y, Wei K, Zou F, Zhong S. Temozolomide loaded PLGA-based superparamagnetic nanoparticles for magnetic resonance imaging and treatment of malignant glioma. *Int J Pharm.* 2012;**430**:266-75. doi: 10.1016/j.ijpharm.2012.03.047. PubMed PMID: 22486964.
 15. Wen PY, Kesari S. Malignant gliomas in adults. *N Engl J Med.* 2008;**359**:492-507. doi: 10.1056/NEJMr0708126. PubMed PMID: 18669428.
 16. Ostrom QT, Gittleman H, Liao P, Rouse C, Chen Y, Dowling J, et al. CBTRUS statistical report: primary brain and central nervous system tumors diagnosed in the United States in 2007-2011. *Neuro Oncol.* 2014;**16** Suppl 4:iv1-63. doi: 10.1093/neuonc/nou223. PubMed PMID: 25304271. PubMed PMCID: PMC4193675.
 17. Fang C, Wang K, Stephen ZR, Mu Q, Kievit FM, Chiu DT, et al. Temozolomide nanoparticles for targeted glioblastoma therapy. *ACS Appl Mater Interfaces.* 2015;**7**:6674-82. doi: 10.1021/am5092165. PubMed PMID: 25751368. PubMed PMCID: PMC4637162.
 18. Walker MD, Strike TA, Sheline GE. An analysis of dose-effect relationship in the radiotherapy of malignant gliomas. *Int J Radiat Oncol Biol Phys.* 1979;**5**:1725-31. PubMed PMID: 231022.
 19. Ruben JD, Dally M, Bailey M, Smith R, McLean CA, Fedele P. Cerebral radiation necrosis: incidence, outcomes, and risk factors with emphasis on radiation parameters and chemotherapy. *Int J Radiat Oncol Biol Phys.* 2006;**65**:499-508. doi: 10.1016/j.ijrobp.2005.12.002. PubMed PMID: 16517093.
 20. Lu AH, Salabas EL, Schuth F. Magnetic nanoparticles: synthesis, protection, functionalization, and application. *Angew Chem Int Ed Engl.* 2007;**46**:1222-44. doi: 10.1002/anie.200602866. PubMed PMID: 17278160.
 21. Kanwar JR, Mahidhara G, Kanwar RK. Recent advances in nanoneurology for drug delivery to the brain. *Current nanoscience.* 2009;**5**:441-8.
 22. Pankhurst QA, Connolly J, Jones S, Dobson J. Applications of magnetic nanoparticles in biomedicine. *Journal of physics D: Applied physics.* 2003;**36**:R167.
 23. Chertok B, Moffat BA, David AE, Yu F, Bergemann C, Ross BD, et al. Iron oxide nanoparticles as a drug delivery vehicle for MRI monitored magnetic targeting of brain tumors. *Biomaterials.* 2008;**29**:487-96. doi: 10.1016/j.biomaterials.2007.08.050. PubMed PMID: 17964647. PubMed PMCID: PMC2761681.
 24. Hadjipanayis CG, Machaidze R, Kaluzova M, Wang L, Schuette AJ, Chen H, et al. EGFRvIII antibody-conjugated iron oxide nanoparticles for magnetic resonance imaging-guided convection-enhanced delivery and targeted therapy of glioblastoma. *Cancer Res.* 2010;**70**:6303-12. doi: 10.1158/0008-5472.CAN-10-1022. PubMed PMID: 20647323. PubMed PMCID: PMC2912981.
 25. Braun S, Oppermann H, Mueller A, Renner C, Hovhannisyan A, Baran-Schmidt R, et al. Hedgehog signaling in glioblastoma multiforme. *Cancer Biol Ther.* 2012;**13**:487-95. doi: 10.4161/cbt.19591. PubMed PMID: 22406999.
 26. Huang FK, Chen WC, Lai SF, Liu CJ, Wang CL, Wang CH, et al. Enhancement of irradiation effects on cancer cells by cross-linked dextran-coated iron oxide (CLIO) nanoparticles. *Phys Med Biol.* 2010;**55**:469-82. doi: 10.1088/0031-9155/55/2/009. PubMed PMID: 20023329.
 27. Klein S, Sommer A, Distel LV, Neuhuber W, Kryschi C. Superparamagnetic iron oxide nanoparticles as radiosensitizer via enhanced reactive oxygen species formation. *Biochem Biophys Res Commun.* 2012;**425**:393-7. doi: 10.1016/j.bbrc.2012.07.108. PubMed PMID: 22842461.
 28. Roeske JC, Nunez L, Hoggarth M, Labay E, Weichselbaum RR. Characterization of the theoretical radiation dose enhancement from nanoparticles. *Technol Cancer Res Treat.* 2007;**6**:395-401. doi: 10.1177/153303460700600504. PubMed PMID: 17877427.
 29. Veisoh O, Sun C, Gunn J, Kohler N, Gabikian P, Lee D, et al. Optical and MRI multifunctional nanoprobe for targeting gliomas. *Nano Lett.* 2005;**5**:1003-8. doi: 10.1021/nl0502569. PubMed PMID: 15943433.
 30. Hu F, Neoh KG, Cen L, Kang ET. Cellular response to magnetic nanoparticles "PEGylated" via surface-initiated atom transfer radical polymerization. *Biomacromolecules.* 2006;**7**:809-16. doi: 10.1021/bm050870e. PubMed PMID: 16529418.
 31. Lutz JF, Stiller S, Hoth A, Kaufner L, Pison U, Cartier R. One-pot synthesis of pegylated ultrasmall iron-oxide nanoparticles and their in vivo evaluation as magnetic resonance imaging contrast agents. *Biomacromolecules.* 2006;**7**:3132-8. doi: 10.1021/bm0607527. PubMed PMID: 17096542.
 32. Frey H. Hyperbranched polyglycerols (Synthesis and Applications). *Encyclopedia of Polymeric Nanomaterials.* 2015:977-80.
 33. Saucier-Sawyer JK, Deng Y, Seo YE, Cheng CJ, Zhang J, Quijano E, et al. Systemic delivery of blood-brain barrier-targeted polymeric nanoparticles enhances delivery to brain tissue. *J Drug Target.* 2015;**23**:736-49. doi: 10.3109/1061186X.2015.1065833. PubMed PMID: 26453169. PubMed PMCID: PMC4860350.
 34. Deng Y, Saucier-Sawyer JK, Hoimes CJ, Zhang J, Seo YE, Andrejcsk JW, et al. The effect of hyperbranched polyglycerol coatings on drug delivery using degradable polymer nanoparticles. *Biomaterials.* 2014;**35**:6595-602. doi: 10.1016/j.biomaterials.2014.04.038. PubMed PMID: 24816286. PubMed PMCID: PMC4062180.
 35. Maity D, Choo S-G, Yi J, Ding J, Xue JM. Synthesis

- of magnetite nanoparticles via a solvent-free thermal decomposition route. *Journal of Magnetism and Magnetic Materials*. 2009;**321**:1256-9.
36. Zhao L, Chano T, Morikawa S, Saito Y, Shiino A, Shimizu S, et al. Hyperbranched polyglycerol-grafted superparamagnetic iron oxide nanoparticles: synthesis, characterization, functionalization, size separation, magnetic properties and biological applications. *Advanced Functional Materials*. 2012;**22**:5107-17.
 37. Indira T, Lakshmi P. Magnetic nanoparticles—a review. *Int J Pharm Sci Nanotechnol*. 2010;**3**:1035-42.
 38. Mody VV, Cox A, Shah S, Singh A, Bevins W, Parihar H. Magnetic nanoparticle drug delivery systems for targeting tumor. *Applied Nanoscience*. 2014;**4**:385-92.
 39. Han L, Shi S, Gong T, Zhang Z, Sun X. Cancer stem cells: therapeutic implications and perspectives in cancer therapy. *Acta Pharmaceutica Sinica B*. 2013;**3**:65-75.
 40. Kratzke RA, Kramer BS. Evaluation of in vitro chemosensitivity using human lung cancer cell lines. *J Cell Biochem Suppl*. 1996;**24**:160-4. PubMed PMID: 8806098.
 41. Franken NA, Rodermond HM, Stap J, Haveman J, Van Bree C. Clonogenic assay of cells in vitro. *Nat Protoc*. 2006;**1**:2315-9. doi: 10.1038/nprot.2006.339. PubMed PMID: 17406473.
 42. Buch K, Peters T, Nawroth T, Sanger M, Schmidberger H, Langguth P. Determination of cell survival after irradiation via clonogenic assay versus multiple MTT Assay-A comparative study. *Radiation oncology*. 2012;**7**:1.
 43. Chou T, Martin N. CompuSyn software for drug combinations and for general dose-effect analysis and user's guide. Paramus: ComboSyn Inc; 2007.
 44. Tartaj P, Serna CJ. Synthesis of monodisperse superparamagnetic Fe/silica nanospherical composites. *J Am Chem Soc*. 2003;**125**:15754-5.
 45. Marinin A. Synthesis and characterization of superparamagnetic iron oxide nanoparticles coated with silica. School of Information and Communication Technology Royal Institute of Technology: Stockholm; 2012.
 46. Keshavarzi E, Ghaeb Y, Rouhani SF. The magnetic properties of Fe₃O₄ nanoparticale with different Coats and hydrodynamic diameters. c2010. Available From: http://www.civilica.com/Paper-ISPTC12-ISPTC12_121.html.
 47. Wang L, Neoh K, Kang E, Shuter B, Wang SC. Superparamagnetic hyperbranched polyglycerol-grafted Fe₃O₄ nanoparticles as a novel magnetic resonance imaging contrast agent: an in vitro assessment. *Advanced Functional Materials*. 2009;**19**:2615-22.
 48. Ankamwar B, Lai T-C, Huang J-H, Liu R-S, Hsiao M, Chen C-H, et al. Biocompatibility of Fe₃O₄ nanoparticles evaluated by in vitro cytotoxicity assays using normal, glia and breast cancer cells. *Nanotechnology*. 2010;**21**:075102.
 49. Choi JY, Lee SH, Na HB, An K, Hyeon T, Seo TS. In vitro cytotoxicity screening of water-dispersible metal oxide nanoparticles in human cell lines. *Bioprocess Biosyst Eng*. 2010;**33**:21-30. doi: 10.1007/s00449-009-0354-5. PubMed PMID: 19636592.
 50. Mahmoudi M, Hofmann H, Rothen-Rutishauser B, Petri-Fink A. Assessing the in vitro and in vivo toxicity of superparamagnetic iron oxide nanoparticles. *Chem Rev*. 2012;**112**:2323-38. doi: 10.1021/cr2002596. PubMed PMID: 22216932.
 51. Harvey KA, Xu Z, Saaddatzadeh MR, Wang H, Pollok K, Cohen-Gadol AA, et al. Enhanced anticancer properties of lomustine in conjunction with docosahexaenoic acid in glioblastoma cell lines. *J Neurosurg*. 2015;**122**:547-56. doi: 10.3171/2014.10.JNS14759. PubMed PMID: 25526274.
 52. Sutradhar KB, Amin ML. Nanotechnology in cancer drug delivery and selective targeting. *ISRN Nanotechnology*. 2014;**2014**.
 53. Saatchi K, Gelder N, Gershkovich P, Sivak O, Wasan KM, Kainthan RK, et al. Long-circulating non-toxic blood pool imaging agent based on hyperbranched polyglycerols. *Int J Pharm*. 2012;**422**:418-27. doi: 10.1016/j.ijpharm.2011.10.036. PubMed PMID: 22044540.
 54. Tubiana M, Introduction to radiobiology. Florida: CRC Press; 2005.
 55. Hall EJ, Giaccia AJ. Radiobiology for the Radiologist. Philadelphia: Lippincott Williams & Wilkins; 2006.
 56. Ott M, Gogvadze V, Orrenius S, Zhivotovsky B. Mitochondria, oxidative stress and cell death. *Apoptosis*. 2007;**12**:913-22. doi: 10.1007/s10495-007-0756-2. PubMed PMID: 17453160.
 57. Jia HY, Liu Y, Zhang XJ, Han L, Du LB, Tian Q, et al. Potential oxidative stress of gold nanoparticles by induced-NO releasing in serum. *J Am Chem Soc*. 2009;**131**:40-1. doi: 10.1021/ja808033w. PubMed PMID: 1907265.
 58. Klein S, Dell'Arciprete ML, Wegmann M, Distel LV, Neuhuber W, Gonzalez MC, et al. Oxidized silicon nanoparticles for radiosensitization of cancer and tissue cells. *Biochem Biophys Res Commun*. 2013;**434**:217-22. doi: 10.1016/j.bbrc.2013.03.042. PubMed PMID: 23535374.
 59. Misawa M, Takahashi J. Generation of reactive oxygen species induced by gold nanoparticles under x-ray and UV Irradiations. *Nanomedicine*. 2011;**7**:604-14. doi: 10.1016/j.nano.2011.01.014. PubMed PMID: 21333754.
 60. Gara PMD, Garabano NI, Portoles MJL, Moreno MS, Dodat D, Casas OR, et al. ROS enhancement by silicon nanoparticles in X-ray irradiated aqueous suspensions and in glioma C6 cells. *J Nanopart Res*. 2012;**14**:741.
 61. Lehnert S. Radiosensitizers and Radiochemotherapy in the Treatment of Cancer. New York: CRC Press; 2014.